

HGR-Net: A Fusion Network for Hand Gesture Segmentation and Recognition

Amirhossein Dadashzadeh¹, Alireza Tavakoli Targhi^{2*}, Maryam Tahmasbi², Majid Mirmehdi¹

Department of Computer Science, University of Bristol, Bristol, UK¹

Department of Computer Science, Shahid Beheshti University, Tehran, Iran²

Abstract

We propose a two-stage convolutional neural network (CNN) architecture for robust recognition of hand gestures, called HGR-Net, where the first stage performs accurate semantic segmentation to determine hand regions, and the second stage identifies the gesture. The segmentation stage architecture is based on the combination of fully convolutional residual network and atrous spatial pyramid pooling. Although the segmentation sub-network is trained without depth information, it is particularly robust against challenges such as illumination variations and complex backgrounds. The recognition stage deploys a two-stream CNN, which fuses the information from the red-green-blue and segmented images by combining their deep representations in a fully connected layer before classification. Extensive experiments on public datasets show that our architecture achieves almost as good as state-of-the-art performance in segmentation and recognition of static hand gestures, at a fraction of training time, run time, and model size. Our method can operate at an average of 23 ms per frame.

1 Introduction

Gestures are an integral part of social interaction which can help us to convey information and express our thoughts and feelings more effectively. Hand gestures enable an intuitive and natural means of connection between humans, and can also serve well for interaction between humans and machines. Indeed, recognizing hand gestures has long been an active area of research in visual pattern analysis with a wide range of applications, including human-computer interaction [1], sign language communication [2, 3], virtual reality [4].

Hand Gesture Recognition (HGR) has been tackled by wearable sensors [5] and vision sensors [6, 1] to identify static and/or dynamic gestures. A vision-based approach is preferable as it offers a remote, contact-free and still affordable HGR system. The traditional methods from the pre-deep learning era used hand-crafted shape and appearance features for static gestures [7], and added motion features to recognize dynamic gestures in video sequences [8, 9, 10]. Recently, deep learning models have achieved great success in a wide range of computer vision tasks, including image classification [11], object detection [12] and semantic segmentation [13, 14]. These successes have motivated many researchers to develop HGR systems based on deep learning algorithms [15, 16, 17].

An important preprocessing step in HGR is the segmentation of hand regions - a highly challenging task, due to the variability of the image background, ethnicity color differences, shadows, and other illumination variations. One potential solution to deal with such difficulties is to use depth sensors, such as the Microsoft Kinect [18]. However, depth-sensing devices might not be suitable for all environments, especially in outdoor scenarios, and add to the computational burden.

In this paper, we propose a novel HGR system using a deep learning framework, where we design a two-stage convolutional neural network (CNN) architecture for segmentation and recognition of hand gestures. An overview of the network is shown in Fig. 1.

At the first stage of the network, a deep architecture based on fully convolutional residual network is used to segment the hand out of the image. This stage adopts an Atrous Spatial Pyramid Pooling (ASPP) module [19], which encodes global contextual information at multiple scales. In the second stage, we build a two-stream CNN to learn feature representations for the input RGB images and their corresponding hand segmentation maps from the first stage separately, which are then combined with a late fusion ap-

*a_tavakoli@sbu.ac.ir

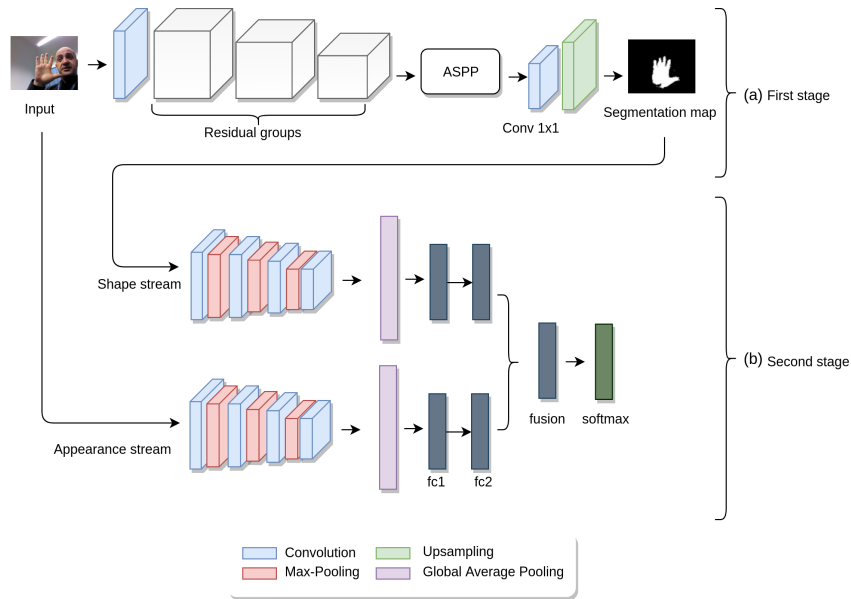


Figure 1: The proposed HGR-Net: (a) a hand segmentation network is first trained to segment hand regions from the background, (b) a shape stream and an appearance stream are then trained separately to capture corresponding information, which are then combined in a fusion layer before a softmax classifier.

proach. This architecture bears similarity to other recent multi-stream CNNs [20, 21, 22]. However, in this work we consider the relationship between the RGB images and the segmentation map, instead of requiring multimodal RGB and depth or motion (optical flow). The main advantage of this two-stage architecture is that it exploits the RGB image and the segmentation map at training time, and recognizes the hand directly from only the 2D RGB frames at testing time, with an average processing rate of 23ms per frame.

To improve the generalization capability of HGR-Net significantly, we present an efficient data augmentation strategy by employing both online and offline data augmentation. The proposed method is evaluated on two benchmark datasets, i.e. OUHANDS [23] and HGR1 [24]. Our experiments show that by using a robust hand segmentation/recognition architecture, supported by an efficient data augmentation technique, we can develop a robust RGB-based HGR system which has excellent performance in uncontrolled and unseen scenarios, at much lower training and computational costs than the current state of the art¹.

Next, in Section 2, we describe related works. In Section 3, our proposed methodology, encapsulating the design of HGR-Net, is outlined. The experimental results are discussed in Section 4, and finally we conclude the paper in Section 5.

¹The code and trained models of our paper will be made available on github.

2 Related Works

Hand Segmentation - Segmentation of hands plays an important role in many computer vision applications, such as hand tracking [25], hand pose estimation [26] and gesture recognition [1]. In recent years, skin segmentation has been widely used by several approaches for hand segmentation [27, 28, 29]. Among such works color-based methods have been popular with many applying threshold-based techniques on different color spaces to achieve the best skin segmentation performance [30, 31, 32].

Machine learning techniques for skin segmentation, such as [27, 33, 34] utilize a classifier trained on skin (hand) and non-skin (background) classes. In [35, 36], Kawulok and co-workers extracted textural features from skin probability maps and then propagated them in a spatial analysis scheme. Hettiarachchi and Peters [37] built their skin classifier training data set with skin and skin-like classes instead of skin and non-skin classes in order to obtain a more balanced class distribution in the training dataset. They segmented the skin candidate regions using a Voronoi-based image segmentation technique and then classified them using a multi-manifold-based skin classifier.

These previous approaches have significant drawbacks in that they do not perform well when the background color is similar to skin color, and that they are seriously affected by lighting conditions.

To overcome such limitations, many works have taken advantage of depth information, such as [38, 39, 25, 40]. For example, Kang *et al.* [40] proposed a two-stage random decision forest (RDF) classifier, where the first stage detects

hands by processing the RDF on an entire depth map, and the second stage segments hands by applying the RDF in the detected regions.

Hand Gesture Recognition - Numerous methods for recognizing hand gestures in static images have been proposed over the years, e.g [41, 7, 15]. Among traditional feature-based methods, Pisharady *et al.* [41] utilized a Bayesian model of visual attention to identify hand regions within images. Hand gestures were recognized using low level (color) and high level (shape, texture) features of the hand areas, with a Support Vector Machines (SVM) classifier. Priyal and Bora [42] used geometry based normalizations and Krawtchouk moment features to represent binary silhouettes of hands in a rotation invariant manner. Nalepa *et al.* [28] proposed a parallel algorithm for hand shape classification which performed in real-time over the segmented hand gestures. They combined shape contexts with appearance-based techniques to increase the classification score. A combination of graph-based characteristics and shape-based features, such as Canny edges, was proposed by Avraam [43] for modeling static hand gestures.

Depth cameras have also been applied to the HGR problem, e.g. [39, 44, 45, 7]. In [44], the authors combined depth features and skeletal data descriptors using Leap Motion and Kinect devices. An SVM classifier with a Gaussian radial basis function kernel was then used to recognize the performed gestures. In [7], the k-curvature algorithm was employed to describe hand poses through extracted contours. Then, a dynamic time warping algorithm was used for recognition, where the gesture under analysis was compared with a series of pre-recorded reference gestures. This technique was used for the classification of static and dynamic hand gestures.

Deep learning-based methods - Barros *et al.* [46] developed a convolutional neural network for hand pose analysis with three channels, where one takes a gray-scale image and the second and third receive the edge maps resulting from the application of the Sobel filter in horizontal and vertical directions, respectively.

Liang *et al.* [47] proposed a multi-view framework for recognizing hand gestures using point clouds captured by a depth sensor. They used CNNs as feature extractors and finally employed an SVM classifier to classify hand gestures. Oyedotun and Khashman [17] utilized a CNN and stacked denoising autoencoder for recognizing 24 American Sign Language hand gestures. They evaluated their recognition performance on a public database, which was collected under controlled background and lighting conditions, reaching recognition rates of 91.33% and 92.83% by models called CNN1 and SDAE3, respectively. Recently, Chevchenko *et al.* [15] presented a new architecture based on the combination of a CNN and traditional feature extractors including Hu moments, Gabor filters and Zernike moments. The au-

thors evaluated their method on binary, depth and grayscale images, using data where the background was either already removed or ignored by operating on the hand as the closest object to the camera. Moreover, their experimental results on the OUHANDS dataset [23] cannot really represent the generalization capacity of their model, since they apply a leave-one-out cross validation approach on the entire dataset that contains training, validation, and test sets. Finally, their method cannot be directly compared against as they do not report their results on the standard test set of the dataset.

In conclusion, there is still a lack of a highly accurate solution to the problem of non-depth based, static, hand gesture recognition in uncontrolled environments. In this article, we address this issue by proposing a two-stage CNN architecture, which enables the full exploitation of the shape and appearance information from single RGB images.

3 Proposed Method

The structure of the proposed HGR-Net is shown in Fig. 1. In summary, the network consists of three CNNs, operating over two stages. In the first stage, the candidate hand regions are segmented in the RGB image and used as input to the second stage (Section 3.1). The second stage is composed of two streams, one for the input RGB image and one for the segmentation map from the first stage (Section 3.2). Each of the streams consists of a deep CNN which are converged in a fully-connected layer and a softmax classifier. To train the HGR-Net, we proceed in a stage-wise manner which is common practice in multi-stream architectures (Section 3.3).

3.1 Hand Segmentation

Most deep learning techniques that have been successfully used for semantic segmentation are based on Fully Convolutional Networks (FCN) [13, 19]. The main idea in FCN-based networks is that they remove fully-connected layers to create an efficient end-to-end learning algorithm. In this work, we take advantage of this idea to build a powerful deep network for hand segmentation. Our network, explained in detail below, consists of two main parts: (1) a deep fully convolutional residual network for learning useful representations, and (2) an ASPP module to encode multi-scale context by adopting multiple dilation rates.

Fully convolutional residual network - Theoretically, increasing network depth should increase the capacity and representation of the network [48]. However, in practice this is impossible due to many limitations, such as the risk of overfitting, vanishing gradients, and difficulty in efficient optimization. So increasing network layers to make

a deeper network does not work by simply stacking layers together. To overcome these problems, He *et al.* [49] proposed a residual learning technique to ease the training of networks that enables them to be substantially deeper. This technique allows gradients to flow across multiple layers during the training process by using identity mappings as skip connections. We take advantage of residual learning to construct a deep CNN with 28 convolution layers. As shown in Fig. 1(a) and Table 1, we consider 3 residual

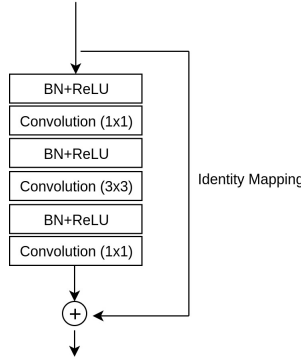


Figure 2: The structure of residual unit with bottleneck used in the proposed method. BN denotes Batch Normalization.

groups where each group contains 3 residual units, stacked together. The structure of these units is shown in Fig. 2. Each unit can be defined as

$$y_k = h(x_k) + F(x_k; W_k), \quad (1)$$

where x_k and y_k represent the input and output of the k^{th} unit, $h(x_k)$ is an identity mapping and F is the residual function defined by weights W_k .

As seen in Fig. 2, we use a bottleneck architecture for each residual unit with two 1×1 convolution layers. This architecture reduces the dimensionality and then restores it. The downsampling operation is performed by the first 1×1 convolution in the second and third residual groups with a stride of 2.

Atrous Spatial Pyramid Pooling - Contextual information has been shown to be extremely important for semantic segmentation tasks [50, 51]. In a CNN, the size of the receptive field can roughly determine how much we need to capture context. Although the wider receptive field allows us to gather more context, Zhou *et al.* [52] showed that the actual size of the receptive fields in a CNN is much smaller than the theoretical size, especially in higher level layers. To solve this problem, Yu and Koltun [53] proposed atrous convolution which can exponentially enlarge the receptive field to capture long-range context without losing spatial resolution and increasing the number of parameters.

We combine different scales of contextual information using an ASPP module as shown in Fig. 3. This kind of

module has been employed successfully in the state-of-the-art DeepLabv3 [19] for semantic segmentation. The ASPP module used in this work has five levels, a 1×1 convolution and four 3×3 convolutions with atrous rates of 1, 3, 6, 12 and 18 respectively (all with 32 filters). The resulting five feature maps are concatenated together. Then, the output from the concatenation unit is fed to a 1×1 convolution and is upsampled by a standard 4x bilinear interpolation to provide an end-to-end learning algorithm for hand segmentation (see Fig. 1(a)).

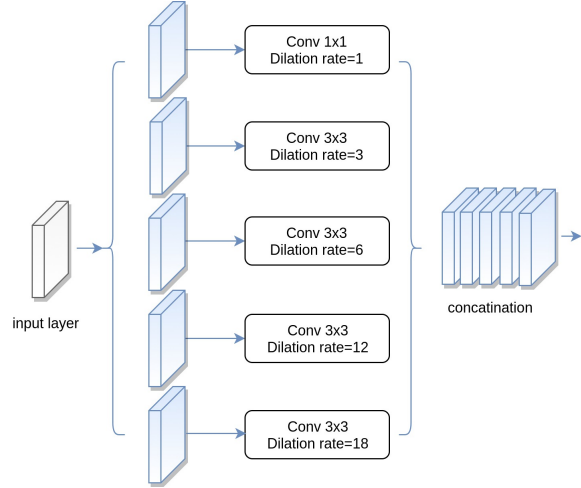


Figure 3: The structure of our ASPP module with 5 parallel operations.

3.2 Hand Gesture Recognition

In this stage of our proposed method, we predict the hand gesture label using a fusion of two CNNs. As shown in Fig. 1(b), this stage consists of two separate CNNs with the same architecture where each network exploits the shape-based and appearance-based information respectively, conveyed

Table 1 Our fully convolutional residual network architecture with 28 convolution layers in the first stage of HGR-Net.

Layer name	Output shape	Layers
input	$320 \times 320 \times 3$	
convolution	$320 \times 320 \times 16$	
ResGroup1	$320 \times 320 \times 32$	$\begin{bmatrix} 1 & 1 & 8 \\ 3 & 3 & 8 \\ 1 & 1 & 32 \end{bmatrix} \times 3$
ResGroup2	$160 \times 160 \times 64$	$\begin{bmatrix} 1 & 1 & 16 \\ 3 & 3 & 16 \\ 1 & 1 & 64 \end{bmatrix} \times 3, \text{ stride}=2$
ResGroup3	$80 \times 80 \times 128$	$\begin{bmatrix} 1 & 1 & 32 \\ 3 & 3 & 32 \\ 1 & 1 & 128 \end{bmatrix} \times 3, \text{ stride}=2$

by the hand segmentation map from the previous stage and the RGB image for robust hand gesture recognition. Each CNN consists of several operations including convolution, pooling and ReLUs, followed by two fully-connected layers at the end of the network. The detailed structure of these CNNs is shown in Table 2.

A fusion function is then deployed to fuse the outputs of the last fully-connected layer of each network in an element-wise summation manner. More formally, let $f^S \in \mathbb{R}^d$ and $f^A \in \mathbb{R}^d$ be the outputs of the last fully connected layers (fc2) from the first (shape stream) and second (appearance stream) CNN respectively. The output of the fusion function f^{sum} is

$$f_i^{sum} = f_i^S + f_i^A, \quad (2)$$

where $1 \leq i \leq d$ and $f^{sum} \in \mathbb{R}^d$, and d is number of the neurons (in our experiments 64 for fc2). The feature vector f^{sum} is then fed into a softmax classifier for joint supervised learning. It is worth noting that, since our model benefits from a segmentation, it takes the RGB image as the only input at testing time.

3.3 Training Paradigm

Let $S = \{(\mathbf{x}_i, \mathbf{m}_i, \mathbf{y}_i) \text{ for } i = 1, \dots, N\}$ be the N training samples where $\mathbf{x}_i \in \mathbb{R}^{h \times w \times 3}$, $\mathbf{m}_i \in \mathbb{R}^{h \times w \times 1}$ and $\mathbf{y}_i \in \mathbb{R}^c$ are the RGB images, segmentation masks, and the corresponding image labels in one-hot encoding respectively. The training paradigm of the HGR-Net is divided into three main steps.

1) *Training the segmentation network:* Since the shape stream relies on the hand segmentation map, in the first step we train the hand segmentation network (Fig. 1(a)) using

RGB images (\mathbf{x}_i) and the corresponding hand segmentation masks (\mathbf{m}_i). To find the optimal weights of the segmentation network, we need to minimize,

$$\min_{\theta^{seg}} \frac{1}{N} \sum_{i=1}^N \mathcal{L}(\text{sigmoid}(p^{seg}(\mathbf{x}_i, \theta^{seg})), \mathbf{m}_i), \quad (3)$$

where $\theta^{seg} = \{\mathbf{W}^{seg}, \mathbf{b}^{seg}\}$ are the parameters (weights and biases) of the segmentation network and $p^{seg}(\cdot)$ is the function that maps the \mathbf{x}_i to the class scores \mathbf{s}^{seg} , where $\mathbf{s}^{seg} \in \mathbb{R}^{h \times w \times 1}$. We use the sigmoid function to produce the segmentation probability map by squashing the values of \mathbf{s}^{seg} in the range (0, 1). The loss function $\mathcal{L}(\cdot)$ is defined as

$$\mathcal{L}(\mathbf{p}, \mathbf{y}) = -[\mathbf{y} \log(\mathbf{p}) + (1 - \mathbf{y}) \log(1 - \mathbf{p})], \quad (4)$$

where \mathbf{y} is the true class (in this step $\mathbf{y}=\mathbf{m}_i$), and \mathbf{p} is the predicted probability for that class (in this step $\mathbf{p} = \text{sigmoid}(\mathbf{s}^{seg})$). We use this loss function in all our training steps.

2) *Training the stream networks:* After training the segmentation network, we keep its trained weights to train the shape stream using RGB images (\mathbf{x}_i) and their corresponding one-hot vectors (\mathbf{y}_i). To find the optimal weights of the shape stream network, we need to minimize the loss function \mathcal{L} , described in this step as

$$\min_{\theta^S} \frac{1}{N} \sum_{i=1}^N \sum_{c=1}^C \mathcal{L}(\text{softmax}(p^{rec}(\mathbf{x}_i, \theta^{seg}, \theta^S)), \mathbf{y}_i), \quad (5)$$

where $\theta^S = \{\mathbf{W}^S, \mathbf{b}^S\}$ are the parameters of the shape stream network and $p^{rec}(\cdot)$ is the function that maps the \mathbf{x}_i to the class scores \mathbf{s}^{rec} , where $\mathbf{s}^{rec} \in \mathbb{R}^c$. By using the softmax classifier, we map \mathbf{s}^{rec} to a probability distribution over C classes. In this step, the softmax classifier is replaced with the last fully connected layer (fc2).

We also train the appearance stream in a similar fashion, except that this stream does not rely on the hand segmentation network weights, as shown in Fig. 1(b).

3) *Training the fusion network:* In the last step, we initialize the HGR-Net weights with the weights of the pre-trained CNNs from previous steps and we train the whole network (HGR-Net) by minimizing,

$$\min_{\theta^S, \theta^A, \theta^F} \frac{1}{N} \sum_{i=1}^N \sum_{c=1}^C \mathcal{L}(\text{softmax}(p^{rec}(\mathbf{x}_i, \theta^{seg}, \theta^S, \theta^A, \theta^F)), \mathbf{y}_i), \quad (6)$$

where $\theta^A = \{\mathbf{W}^A, \mathbf{b}^A\}$ and $\theta^F = \{\mathbf{W}^F, \mathbf{b}^F\}$ are the parameters of the appearance stream and fusion network after fusion layer, respectively.

Note that in this step, training can be performed by optimizing only the weights after fc2 layers and the remaining weights can be frozen.

Table 2 The architecture of the CNNs used in the recognition stage (Fig. 1(b)). Note that both CNNs have the same architecture, except that the shape stream CNN uses a one-channel input image.

Layer	Type	Output Shape
input		$320 \times 320 \times 3$
conv1	convolution	$318 \times 318 \times 16$
pool1	max-pooling	$106 \times 106 \times 16$
conv2	convolution	$104 \times 104 \times 32$
pool2	max-pooling	$34 \times 34 \times 32$
conv3	convolution	$32 \times 32 \times 64$
pool3	max-pooling	$10 \times 10 \times 64$
conv4	convolution	$8 \times 8 \times 128$
pool4	global average pooling	128
dropout1	dropout	128
fc1	fully connected	64
dropout2	dropout	64
fc2	fully connected	64

4 Experimental Evaluation

Datasets - To the best of our knowledge, there are currently very few publicly available datasets for static hand gesture analysis that include hand segmentation groundtruth and were captured under challenging situations. For instance, datasets such as Kinect Leap [44] or Senz3D [45] contain complex backgrounds and face-hand occlusions, but they lack segmentation groundtruth and do not provide a sufficient number of subjects. Moreover, these datasets contain depth maps which are not aligned with their corresponding RGB images, making the generation of segmentation annotations from these depth maps unreliable. We evaluate our proposed method on two benchmark datasets:

OUHANDS [23] - This dataset contains 10 different hand gestures from 23 subjects, and is split into training, validation and testing sets with 1200, 400 and 1000 images respectively. All sets come with corresponding segmentation masks. Each set is performed by different subjects and the images were captured under very challenging situations, such as variations in illumination, complex backgrounds and face-hand occlusions with various hand shapes and sizes. We use this dataset to evaluate HGR-Net for both hand segmentation and hand gesture recognition.

HGR1 [24] - This dataset contains 899 RGB images of 12 individuals performing 25 different hand gestures, collected under uncontrolled backgrounds without any face-hand occlusion. We use HGR1 for evaluating our hand segmentation accuracy only for two reasons. First, the database has only relatively few samples per class, hence it is not particularly useful to evaluate our recognition model. Second, as a popular benchmark dataset among traditional hand segmentation works, it serves the purpose for comparing our deep learning segmentation approach against them.

4.1 Experimental setup

The Keras open source deep learning library [54] with a TensorFlow [55] backend was used to implement the proposed method. As explained in Section 3.3, we trained our HGR-Net in three main steps. For each step, we adopted the same hyperparameters, excluding batch size and dropout rates. We used cross-entropy loss (Eq. 4) as the cost functions, and applied the Adam optimization algorithm [56] to minimize it. The learning rate is initialized as 0.001, and $\beta_1 = 0.9$ and $\beta_2 = 0.999$. We set the mini-batch size as 8 for the first step (training the segmentation network) and 2 for the other steps. The dropout rates for each training step are summarized in Table 3.

The proposed framework was trained using an Nvidia GTX 1080TI GPU with 3.00GHz 4-core CPU and 16GB RAM, under Cuda 9.0 with cuDNN 7.0.5 on TensorFlow

Table 3 Dropout rates for each training step of HGR-Net.

Layer	Training	Dropout Rate Description	Rate
dropout1	Step 1	before Conv 1×1	0.20
dropout2	Step 2	before fc1 layer (both stream networks)	0.20
dropout3	Step 2	after fc1 layer (both stream networks)	0.30
dropout4	Step 3	after fc2 layer (appearance stream)	0.75
dropout5	Step 3	after fc2 layer (shape stream)	0.45
dropout6	Step 3	after fusion layer	0.45

GPU 1.5.0. The maximum number of epochs for each training step was fixed at 150, and the model with the best validation accuracy was selected and used for evaluation. The training time was around 12 hours for all steps. Our trained HGR-Net takes roughly 23ms for a 320×320 input RGB frame. This shows that our model has the potential for real-time implementation.

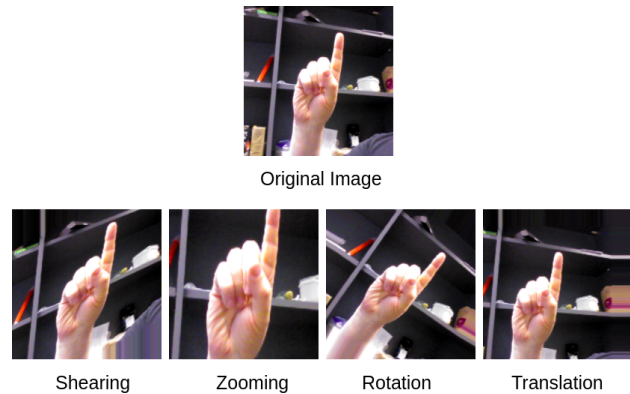


Figure 4: The transformations of the original data used in online data augmentation.

4.2 Data Augmentation

To address the problem of dataset bias, we apply both online and offline data augmentation to prevent overfitting and to improve the model generalization. Our offline data augmentation consists of two transformations: zooming (15%-20%) and vertical/horizontal translations (15%-20%). With these operations, we increase the training set 4-fold.

In online data augmentation, we augment data during training by applying rotation, shearing, zooming, and vertical/horizontal translations (Fig. 4). All of these operations are applied randomly inside the mini-batches that are fed

Table 4 Transformation values for online data augmentation during the training steps.

	rotation	shearing	zooming	translation
stream networks	$\pm 36^\circ$	20%	$\pm 10\%$	2%
HGR-Net	$\pm 41^\circ$	25%	$\pm 15\%$	15%

into the model. The specified value for each transformation is shown in Table 4. Since we train our shape and appearance stream networks from scratch, we adopt lower transformation values for these steps which helps the models to converge faster.

4.3 Experiments on Hand Segmentation

We evaluated our hand segmentation model on OUHANDS [23] and HGR1 [24] datasets. To carry out a quantitative comparison of accuracy of the proposed method, we measure *F-score* which is the equally weighted average of the precision and recall.

First, we evaluate the performance of the segmentation stage of HGR-Net (Stage 1) with and without the ASPP module. We also employ the original architectures of FCN-8s [13], PSPNet [57], and DeepLabv3 [19], to compare their performance with our segmentation model on this specific task. The results are reported in Table 5. We observe that our model works better when used in conjunction with the ASPP module, which is approximately as accurate as DeepLab3 and PSPNet, while being much smaller and 2X faster at run-time for a 320×320 RGB image. We use ResNet-50 [49] as feature extractor for both DeepLabv3 and PSPNet architectures. Our model also slightly outperforms FCN-8s, while also being much smaller and 3X faster. Our proposed model requires the least amount of training time in comparison to all the other networks in Table 5 given the fraction of parameters that need to be trained.

To demonstrate the efficacy of our model qualitatively, some comparative segmentation results on the OUHANDS test set are illustrated in Fig. 5. The images show that our segmentation model deals well with common challenges in hand segmentation, such as uncontrolled backgrounds and lighting conditions.

We further use the HGR1 dataset to compare our hand segmentation model against state-of-the-art methods which are based on traditional feature extraction. To evaluate our model on HGR1, we use 3-fold cross-validation. In each fold, we randomly select 66% of the images for training and the rest for validation. We also perform offline data augmentation (Section 4.2) on each training set and increase them 4-fold. As shown in Table 6, HGR-Net (stage 1) outperforms these traditional methods while it obtains a very

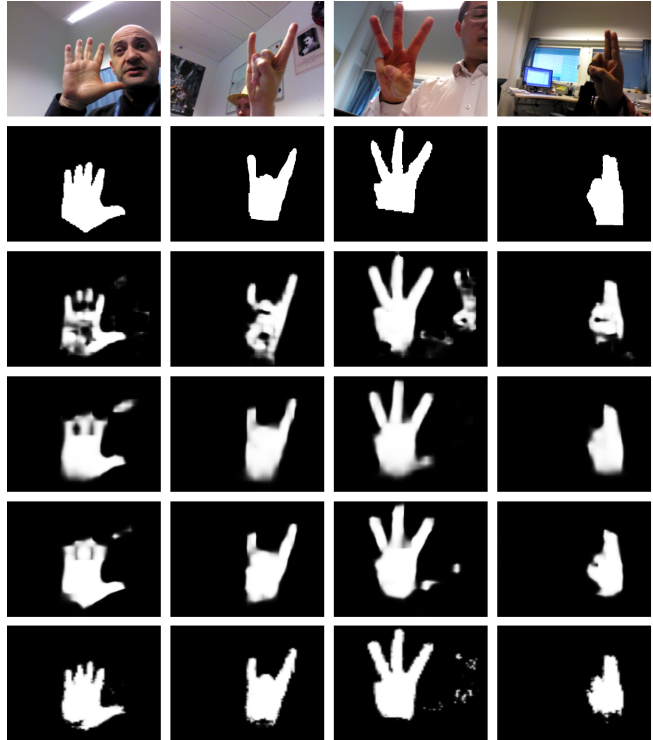


Figure 5: Example segmentations on OUHANDS test set: (top to bottom rows) Input images, ground truth, FCN-8s [13], PSPNet [57], DeepLabv3 [19], and HGR-Net (Stage 1).

comparable performance against DeepLabv3 and PSPNet at a fraction of the run-time, model size, and number of parameters required.

From the qualitative results shown in Fig. 6, we can see that traditional methods tend to fail in distinguishing skin pixels from skin-like backgrounds due to the limited ability of their low-level, hand-crafted features.

4.4 Experiments on HGR

Next, we evaluate HGR-Net for the task of hand gesture recognition. Table 7 shows the classification scores on the OUHANDS test set with different forms of data augmentation. As evident in Table 7, online augmentation provides higher test accuracy than offline, but the highest test

Table 5 Segmentation results on OUHANDS test set.

Method	<i>F-score</i>	Time (ms)	#Parameters	Model Size
FCN-8s [13]	0.9559	63	134M	537MB
PSPNet [57]	0.9702	50	79.44M	318MB
DeepLabv3 [19]	0.9735	43	75.30M	302MB
HGR-Net (Stage 1-no ASPP)	0.9529	20	0.13M	0.79MB
HGR-Net (Stage1)	0.9630	21	0.28M	1.4MB

Table 6 Segmentation results on HGR1 dataset.

Method	<i>F-score</i>	Time (ms)	#Parameters	Model Size
Hettiarachchi <i>et al.</i> [37]	0.9692	-	-	-
Kawulok <i>et al.</i> [36]	0.9562	-	-	-
Kawulok [35]	0.9086	-	-	-
FCN-8s [13]	0.9772	63	134M	537MB
PSPNet [57]	0.9877	50	79.44M	318MB
DeepLabv3 [19]	0.9883	43	75.30M	302MB
HGR-Net (Stage 1)	0.9825	21	0.28M	1.4MB

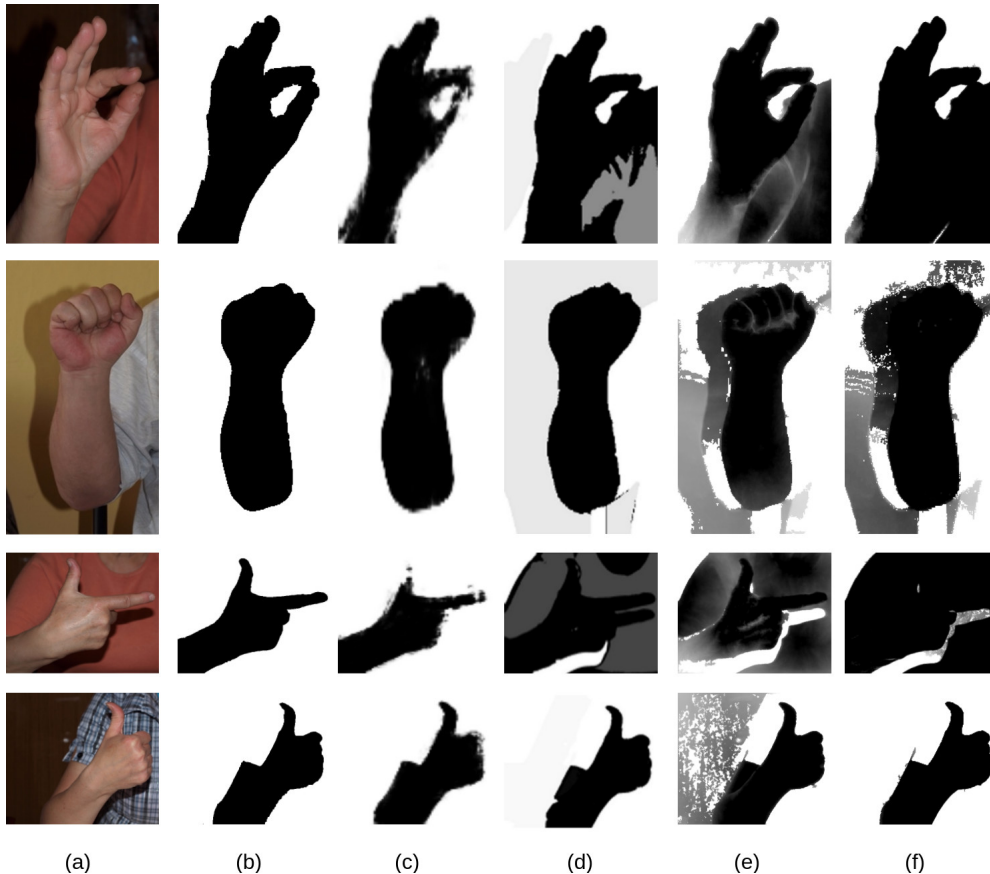


Figure 6: Comparison of segmentation results on HGR1 dataset. (a) Input image, (b) ground truth, (c) HGR-Net (Stage 1). (d) Hettiarachchi et al [37], (e) Kawulok et al, [36], (f) Kawulok [35]. Note, these images were selected from the validation set.

accuracy is achieved when we trained HGR-Net using both offline and online. These results confirm that this data augmentation strategy can significantly reduce overfitting and improves the generalization capability of the model. Hence, it can be useful for robust hand gesture recognition in real-world scenes.

Table 8 compares the performances of different network architectures on the OUHANDS dataset. Rows 1-3 exhibit the influence of each network stream in HGR-Net’s performance. The performance of HGR-Net as a whole then jumps to an F -score of 0.8810 when we apply our late fusion approach to coalesce the shape and appearance streams. This result emphasizes the effectiveness of our fusion network architecture.

Table 7 Evaluation of HGR-Net for hand gesture recognition task with different forms of data augmentation

Data Augmentation	Train	Test (F -score)
None	0.9787	0.7842
Offline	0.9760	0.8165
Online	0.9000	0.8629
Offline+Online	0.8742	0.8810

In rows 4-6 of Table 8, we present the scores of three popular deep architectures, ResNet-50 [49], DenseNet-121 [58] and MobileNet [59], for comparison. For training these networks on the OUHANDS dataset, we only replace their softmax layer, originally trained to recognize 1000 classes, with a softmax layer that recognizes only 10 (i.e. the ten classes in OUHANDS). The weights of other layers are initialized from the original network that was trained on ImageNet [60]. Note that the networks’ layers are not frozen during the training process. It can be seen that our full HGR-net (row 3) outperforms these models, and obtains a 1.6% increment over the next best, i.e. MobileNet, while being 6X smaller and bearing a fraction of its parameters. It is interesting to note that we do not use any large-scale dataset for pre-training our model. This can be useful in real-world applications such as online learning in which the HGR system relies on a limited amount of in-coming training data. Moreover, our lightweight CNN is more feasible to deploy on hardware with limited memory. The proposed approach operates at approximately 43 fps².

The last row of the table reports our model’s performance

²Real-time video demo: <https://youtu.be/-KSNrk5plS0>

Table 8 Comparison of recognition accuracy on OUHANDS test set. Note that for fair comparison we use the proposed data augmentation strategy for training all models considered in the table

#	Model	F-score	Input Size	Time (ms)	#Parameters	Model Size
Input: RGB						
1	HGR-Net (Shape stream only)	0.8527	320×320	22	0.385M	1.9MB
2	HGR-Net (Appearance stream only)	0.7545	320×320	0.7	0.106M	0.45MB
3	HGR-Net	0.8810	320×320	23	0.499M	2.4MB
4	ResNet-50 [49]	0.8138	224×224	25	23.60M	99MB
5	DenseNet-121 [58]	0.8281	224×224	24	7.04M	33MB
6	MobileNet [59]	0.8650	224×224	13	3.22M	16MB
Input: binary						
7	CNN1 [17]	0.8667	32×32	0.3	0.126M	0.51MB
8	HGR-Net (Shape stream, no Stage 1)	0.9375	320×320	0.4	0.106M	0.44MB

on binary hand masks. Since we do not use RGB images in this experiment, we only employ the shape stream without relying on the segmentation maps (i.e no part (a) in Figure 1). As expected, our model then performs better than our model with RGB input (row 3) since it does not deal with image backgrounds in both training and testing. For comparison, we evaluate the performance of CNN1 [17] on OUHANDS. Since CNN1 is a single channel CNN, we train and test this network with only binary hand masks. As seen in rows 7-8 of Table 8, our HGR-Net with binary input outperforms CNN1 by a significant margin of ~6%.

Fig. 7 shows the confusion matrix of the full HGR-Net in terms of recognition accuracy on OUHANDS test set. The column and row indices denote the predicted results and the target classes, respectively.

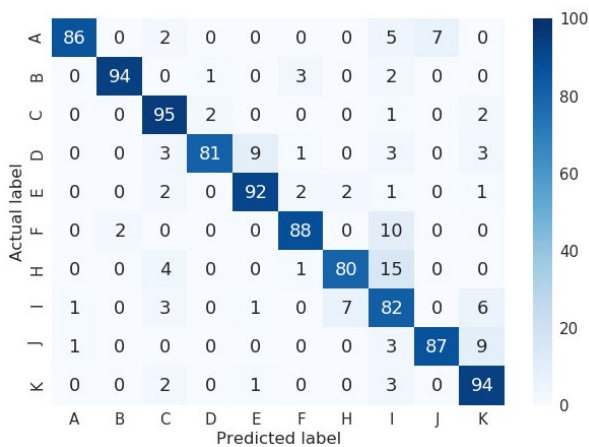


Figure 7: Confusion matrix of the proposed method for hand gesture recognition task on the OUHANDS test set.

5 Conclusion

We presented a two-stage fusion network, based on CNN architecture for the problem of hand gesture recognition. To improve the recognition performance without using depth data, we proposed a hand segmentation architecture in the first stage of the network. Our experimental results showed that our hand segmentation model has a great performance against challenging situations, even when the background color is similar to skin color. For the second stage of the network, we designed a two-stream CNN which can learn to fuse feature representations from both the RGB image and its segmentation map before classification. Moreover, we employed an effective data augmentation technique which plays an important role in obtaining higher recognition accuracy. Our best proposed model achieves state-of-the-art performance on the OUHANDS dataset with a real-time average recognition speed of 23ms per frame or 43 fps. In addition, we evaluated our segmentation model on the HGR1 dataset where it outperformed traditional state-of-the-art methods.

References

- [1] Siddharth S Rautaray and Anupam Agrawal. Vision based hand gesture recognition for human computer interaction: a survey. *Artificial Intelligence Review*, 43(1):1–54, 2015.
- [2] Thad Starner, Joshua Weaver, and Alex Pentland. Real-time american sign language recognition using desk and wearable computer based video. *IEEE Transactions on Pattern Analysis and Machine Intelligence*, 20(12):1371–1375, 1998.

- [3] Helen Cooper, Brian Holt, and Richard Bowden. Sign language recognition. In *Visual Analysis of Humans*, pages 539–562. Springer, 2011.
- [4] Deyou Xu. A neural network approach for hand gesture recognition in virtual reality driving training system of spg. In *18th International Conference on Pattern Recognition*, volume 3, pages 519–522, Salt Palace Convention Center, Salt Lake City, UT, 2006. IEEE.
- [5] Laura Dipietro, Angelo M Sabatini, Paolo Dario, et al. A survey of glove-based systems and their applications. *IEEE Trans. Systems, Man, and Cybernetics, Part C*, 38(4):461–482, 2008.
- [6] Pramod Kumar Pisharady and Martin Saerbeck. Recent methods and databases in vision-based hand gesture recognition: A review. *Computer Vision and Image Understanding*, 141:152–165, 2015.
- [7] Guillaume Plouffe and Ana-Maria Cretu. Static and dynamic hand gesture recognition in depth data using dynamic time warping. *IEEE Transactions on Instrumentation and Measurement*, 65(2):305–316, 2016.
- [8] Quentin De Smedt, Hazem Wannous, and Jean-Philippe Vandeborre. Skeleton-based dynamic hand gesture recognition. In *Proceedings of the IEEE Conference on Computer Vision and Pattern Recognition Workshops*, pages 1–9, 2016.
- [9] Wei Lu, Zheng Tong, and Jinghui Chu. Dynamic hand gesture recognition with leap motion controller. *Signal Processing Letters*, 23(9):1188–1192, 2016.
- [10] Joyeeta Singha, Amarjit Roy, and Rabul Hussain Laskar. Dynamic hand gesture recognition using vision-based approach for human–computer interaction. *Neural Computing and Applications*, 29(4):1129–1141, 2018.
- [11] Alex Krizhevsky, Ilya Sutskever, and Geoffrey E Hinton. Imagenet classification with deep convolutional neural networks. In *Advances in Neural Information Processing Systems*, pages 1097–1105, 2012.
- [12] Shaoqing Ren, Kaiming He, Ross Girshick, and Jian Sun. Faster r-cnn: Towards real-time object detection with region proposal networks. In *Advances in Neural Information Processing Systems*, pages 91–99, 2015.
- [13] Jonathan Long, Evan Shelhamer, and Trevor Darrell. Fully convolutional networks for semantic segmentation. In *Proceedings of the IEEE Conference on Computer Vision and Pattern Recognition*, pages 3431–3440, 2015.
- [14] Yanming Guo, Yu Liu, Theodoros Georgiou, and Michael S Lew. A review of semantic segmentation using deep neural networks. *International Journal of Multimedia Information Retrieval*, 7(2):87–93, 2018.
- [15] Sérgio F Chevtchenko, Rafaella F Vale, Valmir Macario, and Filipe R Cordeiro. A convolutional neural network with feature fusion for real-time hand posture recognition. *Applied Soft Computing*, 2018.
- [16] Pavlo Molchanov, Shalini Gupta, Kihwan Kim, and Jan Kautz. Hand gesture recognition with 3d convolutional neural networks. In *Proceedings of the IEEE Conference on Computer Vision and Pattern Recognition Workshops*, pages 1–7, 2015.
- [17] Oyebade K Oyedotun and Adnan Khashman. Deep learning in vision-based static hand gesture recognition. *Neural Computing and Applications*, 28(12):3941–3951, 2017.
- [18] Carlo Dal Mutto, Pietro Zanuttigh, and Guido M Cortelazzo. Time-of-Flight Cameras and Microsoft Kinect, SpringerBriefs in Electrical and Computer Engineering. Springer New York, 2012.
- [19] Liang-Chieh Chen, George Papandreou, Florian Schroff, and Hartwig Adam. Rethinking atrous convolution for semantic image segmentation. *arXiv preprint arXiv:1706.05587*, 2017.
- [20] Andreas Eitel, Jost Tobias Springenberg, Luciano Spinello, Martin Riedmiller, and Wolfram Burgard. Multimodal deep learning for robust rgb-d object recognition. In *Intelligent Robots and Systems, IEEE/RSJ International Conference on*, pages 681–687, 2015.
- [21] Christoph Feichtenhofer, Axel Pinz, and Andrew Zisserman. Convolutional two-stream network fusion for video action recognition. In *Proceedings of the IEEE Conference on Computer Vision and Pattern Recognition*, pages 1933–1941, 2016.
- [22] Hongyuan Zhu, Jean-Baptiste Weibel, and Shijian Lu. Discriminative multi-modal feature fusion for rgb-d indoor scene recognition. In *Proceedings of the IEEE Conference on Computer Vision and Pattern Recognition*, pages 2969–2976, 2016.
- [23] Matti Matilainen, Pekka Sangi, Jukka Holappa, and Olli Silvén. Ouhands database for hand detection and pose recognition. In *Image Processing Theory Tools and Applications, 6th International Conference on*, pages 1–5. IEEE, 2016.

- [24] HGR1. <http://sun.aei.polsl.pl/~mkawulok/gestures/>.
- [25] Chen Qian, Xiao Sun, Yichen Wei, Xiaou Tang, and Jian Sun. Realtime and robust hand tracking from depth. *IEEE Conference on Computer Vision and Pattern Recognition*, pages 1106–1113, 2014.
- [26] Jonathan Tompson, Murphy Stein, Yann Lecun, and Ken Perlin. Real-time continuous pose recovery of human hands using convolutional networks. *ACM Transactions on Graphics*, 33(5):169, 2014.
- [27] Junwei Han, A Sutherland, Hai Wu, et al. Automatic skin segmentation for gesture recognition combining region and support vector machine active learning. In *Proceedings of the 7th International Conference on Automatic Face and Gesture Recognition*, pages 237–242. IEEE Computer Society, 2006.
- [28] Jakub Nalepa and Michal Kawulok. Fast and accurate hand shape classification. In *International Conference: Beyond Databases, Architectures and Structures*, pages 364–373. Springer, 2014.
- [29] Ajjen Joshi, Camille Monnier, Margrit Betke, and Stan Sclaroff. A random forest approach to segmenting and classifying gestures. In *11th IEEE International Conference and Workshops on Automatic Face and Gesture Recognition*, volume 1, pages 1–7, 2015.
- [30] Antonis A Argyros and Manolis IA Lourakis. Real-time tracking of multiple skin-colored objects with a possibly moving camera. In *European Conference on Computer Vision*, pages 368–379. Springer, 2004.
- [31] Michal Kawulok, Jakub Nalepa, and Jolanta Kawulok. Skin detection and segmentation in color images. In *Advances in Low-Level Color Image Processing*, pages 329–366. Springer, 2014.
- [32] Dariusz J Sawicki and Weronika Miziolek. Human colour skin detection in cmyk colour space. *IET Image Processing*, 9(9):751–757, 2015.
- [33] KK Bhoyar and OG Kakde. Skin color detection model using neural networks and its performance evaluation. In *Journal of Computer Science*. Citeseer, 2010.
- [34] Rehanullah Khan, Allan Hanbury, Julian Stöttinger, and Abdul Bais. Color based skin classification. *Pattern Recognition Letters*, 33(2):157–163, 2012.
- [35] Michal Kawulok. Fast propagation-based skin regions segmentation in color images. In *Automatic Face and Gesture Recognition, 10th IEEE International Conference and Workshops on*, pages 1–7, 2013.
- [36] Michal Kawulok, Jolanta Kawulok, and Jakub Nalepa. Spatial-based skin detection using discriminative skin-presence features. *Pattern Recognition Letters*, 41:3–13, 2014.
- [37] R Hettiarachchi and James F Peters. Multi-manifold-based skin classifier on feature space voronoï regions for skin segmentation. *Journal of Visual Communication and Image Representation*, 41:123–139, 2016.
- [38] Jamie Shotton, Andrew Fitzgibbon, Mat Cook, Toby Sharp, Mark Finocchio, Richard Moore, Alex Kipman, and Andrew Blake. Real-time human pose recognition in parts from single depth images. In *Computer Vision and Pattern Recognition*, pages 1297–1304. IEEE, 2011.
- [39] José Manuel Palacios, Carlos Sagiúés, Eduardo Montijano, and Sergio Llorente. Human-computer interaction based on hand gestures using rgb-d sensors. *Sensors*, 13(9):11842–11860, 2013.
- [40] Byeongkeun Kang, Kar-Han Tan, Nan Jiang, Hung-Shuo Tai, Daniel Treffer, and Truong Nguyen. Hand segmentation for hand-object interaction from depth map. In *Signal and Information Processing, IEEE Global Conference on*, pages 259–263, 2017.
- [41] Pramod Kumar Pisharady, Prahlad Vadakkepat, and Ai Poh Loh. Attention based detection and recognition of hand postures against complex backgrounds. *International Journal of Computer Vision*, 101(3):403–419, 2013.
- [42] S Padam Priyal and Prabin Kumar Bora. A robust static hand gesture recognition system using geometry based normalizations and krawtchouk moments. *Pattern Recognition*, 46(8):2202–2219, 2013.
- [43] Marimpis Avraam. Static gesture recognition combining graph and appearance features. *International Journal of Advanced Research in Artificial Intelligence (IJARAI)*, 3(2), 2014.
- [44] Giulio Marin, Fabio Dominio, and Pietro Zanuttigh. Hand gesture recognition with leap motion and kinect devices. In *Image Processing (ICIP), IEEE International Conference on*, pages 1565–1569, 2014.
- [45] Alvise Memo and Pietro Zanuttigh. Head-mounted gesture controlled interface for human-computer interaction. *Multimedia Tools and Applications*, 77(1):27–53, 2018.
- [46] Pablo Barros, Sven Magg, Cornelius Weber, and Stefan Wermter. A multichannel convolutional neural network for hand posture recognition. In *International*

- Conference on Artificial Neural Networks*, pages 403–410. Springer, 2014.
- [47] Chaoyu Liang, Yonghong Song, and Yuanlin Zhang. Hand gesture recognition using view projection from point cloud. In *Image Processing (ICIP), IEEE International Conference on*, pages 4413–4417, 2016.
- [48] Ian Goodfellow, Yoshua Bengio, Aaron Courville, and Yoshua Bengio. *Deep learning*, volume 1. MIT press Cambridge, 2016.
- [49] Kaiming He, Xiangyu Zhang, Shaoqing Ren, and Jian Sun. Deep residual learning for image recognition. In *Proceedings of the IEEE Conference on Computer Vision and Pattern Recognition*, pages 770–778, 2016.
- [50] Carolina Galleguillos and Serge Belongie. Context based object categorization: A critical survey. *Computer Vision and Image Understanding*, 114(6):712–722, 2010.
- [51] Ziwei Liu, Xiao Xiao Li, Ping Luo, Chen-Change Loy, and Xiaoou Tang. Semantic image segmentation via deep parsing network. In *Proceedings of the IEEE International Conference on Computer Vision*, pages 1377–1385, 2015.
- [52] Bolei Zhou, Aditya Khosla, Agata Lapedriza, Aude Oliva, and Antonio Torralba. Object detectors emerge in deep scene cnns. *arXiv preprint arXiv:1412.6856*, 2014.
- [53] Fisher Yu and Vladlen Koltun. Multi-scale context aggregation by dilated convolutions. *arXiv preprint arXiv:1511.07122*, 2015.
- [54] Keras: Deep learning library for theano and tensorflow. <http://keras.io/>.
- [55] TensorFlow. <https://github.com/tensorflow/tensorflow>.
- [56] Diederik P Kingma and Jimmy Ba. Adam: A method for stochastic optimization. *arXiv preprint arXiv:1412.6980*, 2014.
- [57] Hengshuang Zhao, Jianping Shi, Xiaojuan Qi, Xiaogang Wang, and Jiaya Jia. Pyramid scene parsing network. *IEEE Conference on Computer Vision and Pattern Recognition*, pages 6230–6239, 2017.
- [58] Gao Huang, Zhuang Liu, Laurens van der Maaten, and Kilian Q. Weinberger. Densely connected convolutional networks. *IEEE Conference on Computer Vision and Pattern Recognition*, pages 2261–2269, 2017.
- [59] Andrew G Howard, Menglong Zhu, Bo Chen, Dmitry Kalenichenko, Weijun Wang, Tobias Weyand, Marco Andreetto, and Hartwig Adam. Mobilenets: Efficient convolutional neural networks for mobile vision applications. *arXiv preprint arXiv:1704.04861*, 2017.
- [60] Jia Deng, Wei Dong, Richard Socher, Li-Jia Li, Kai Li, and Li Fei-Fei. Imagenet: A large-scale hierarchical image database. In *CVPR*, 2009.